

Investigating the elliptic anisotropy of identified particles in high-multiplicity p–Pb collisions with a multi-phase transport model

Siyu Tang,^{1,*} Liang Zheng,^{2,†} Xiaoming Zhang,^{3,‡} and Renzhuo Wan^{4,5,§}

¹*School of Mathematical and Physical Sciences,
Wuhan Textile University, Wuhan 430200, China*

²*School of Mathematics and Physics, China University of Geosciences (Wuhan), Wuhan 430074, China*

³*Key Laboratory of Quark and Lepton Physics (MOE) and Institute of Particle Physics,
Central China Normal University, Wuhan 430079, China*

⁴*Hubei Key Laboratory of Digital Textile Equipment,
Wuhan Textile University, Wuhan 430200, China*

⁵*School of Electronic and Electrical Engineering,
Wuhan Textile University, Wuhan 430200, China*

(Dated: March 14, 2023)

The elliptic azimuthal anisotropy coefficient (v_2) of identified particles at midrapidity ($|\eta| > 0.8$) is studied in high-multiplicity p–Pb collisions at $\sqrt{s_{NN}} = 5.02$ TeV with a multi-phase transport model (AMPT). The calculations of differential v_2 of light flavor hadrons (pions, kaons, protons and Λ) are firstly extended to wider transverse momentum (p_T) range, up to 8 GeV/c, based on the advanced flow extraction method. We find that the string melting version of AMPT model can provide a nice description of measured p_T -differential v_2 of mesons, while slightly overestimate the baryon v_2 , and the features of mass ordering and baryon-meson grouping at low and intermediate p_T are also observed. In addition, the necessity of including enough parton interactions to generate positive v_2 in small collision systems is also demonstrated in this paper. Furthermore, we test several nonflow subtraction methods in the extraction of final-state particle v_2 and it is observed that the results are sensitive to the selection of baseline in low-multiplicity reference. This work provides further insights into understanding the origin of collective-like behaviors in small collision systems, and has referential value for the future measurements of azimuthal anisotropy.

Keywords: Azimuthal anisotropy, Small collision systems, Nonflow subtraction

I. INTRODUCTION

The main goal of the heavy-ion collisions at ultra-relativistic energies is to study the deconfined state of strongly-interacting matter created at high energy density and temperature, called the quark-gluon plasma (QGP)[1, 2]. One of the important observables to investigate the transport properties of the QGP is the anisotropic flow[3, 4], which is quantified by the flow harmonic coefficients v_n from the Fourier expansion of the azimuthal distribution of produced particles[5, 6], as

$$\frac{dN}{d\varphi} \propto 1 + 2 \sum_{n=1}^{\infty} v_n \cos[n(\varphi - \Psi_n)], \quad (1)$$

where φ is the azimuthal angle of the final-state particle angle and Ψ_n is the symmetry-plane angle in the collision for the n -th harmonic[7, 8]. The second order coefficient, v_2 , referred to elliptic flow, derived by the initial

state spatial anisotropy of the almond-shaped collision overlap region being propagated to the final state momentum space. Its magnitude is sensitive to the basic transport properties of the fireball, like the temperature dependent equation of state and the ratio of shear viscosity over entropy density (η/s)[9, 10].

In past decades, various measurements of elliptic flow in heavy-ion collisions performed at the Relativistic Heavy Ion Collider (RHIC)[11–14] and the Large Hadron Collider (LHC)[15–18] help to build a full paradigm of the strongly-coupled QGP. These studies indicate that the QGP behaves like a nearly perfect fluid according to the comparison between the extracted η/s and hydrodynamic calculations. In addition, wide measurements of p_T -differential elliptic flow for identified particles are performed in ALICE[19, 20]. The observed mass ordering effect (i.e. the heavier particles have smaller elliptic flow than that of lighter particles at same p_T) at low p_T is well described by hydrodynamic calculations, which attributes to the radial expansion of the QGP. While at intermediate p_T , a grouping of v_2 of mesons and baryons is observed, and the v_2 of mesons is less than that of baryons. These behaviours can be explained by the hypothesis that baryon and meson have different production mechanisms through quark coalescence, which was also further investigated by using the number of constituent quarks (NCQ) scaling[21, 22]. In-

* Correspondence email address: tsy@wtu.edu.cn

† Correspondence email address: zhengliang@cug.edu.cn

‡ Correspondence email address: xiaoming.zhang@ccnu.edu.cn

§ Correspondence email address: wanrz@wtu.edu.cn

terestingly such flow-like phenomena are also found in small collision systems, where no QGP is expected to be formed. The long-range double ridge structures were firstly observed for identified light and strange hadrons in high-multiplicity pp and p-Pb collisions by the ALICE, ATLAS and CMS collaborations, associated with the discovery of a significant positive v_2 [23–26]. The observed particle-mass dependence of v_2 is similar to those measured in heavy-ion collisions[26], suggesting a possible common collective origin of them. It is also worth noting that all current flow measurements in small collision systems face the challenges from the subtraction of the nonflow background, i.e. the correlations not related to collectivity rather due to jet correlations and resonance decay. Even many techniques were proposed to suppress the contribution from nonflow, their different influences on the extraction of flow signal are also need to be carefully considered.

Several theoretical explanations, replying either on the initial-state effects or final-state effect, were proposed to understand the origin of such azimuthal anisotropies in small systems. The studies extending the hydrodynamics from large to small systems based on the final-state effects can well describe the v_2 of soft hadrons[27–29], however they are based on a strong assumption that there are enough scatterings between the constituents in small systems. The Color-Glass Condensate (CGC) based models and the IP-Glasma models considering the effect of momentum correlations in the initial state can quantitatively describe some features of collectivity in p-Pb collisions[30, 31], but without distinct conclusions especially for the dependence on collision systems and rapidity. In addition, an approach called parton escape shows that few scatterings can also create enough azimuthal anisotropies, which was investigated with the a multi-phase transport (AMPT)[32, 33]. The v_2 of light hadrons measured in p-Pb collisions are well described in AMPT, where the anisotropic parton escape instead of hydrodynamics plays an important role[33]. In this study, we further extend the AMPT calculations of the p_T -differential v_2 for identified particles (π^\pm , K^\pm , $p(\bar{p})$, $\Lambda(\bar{\Lambda})$) to higher p_T region in p-Pb collisions at 5.02 TeV, in order to systematically test the mass ordering effect and baryon-meson grouping at low- and intermediate- p_T , respectively. We also investigate that how the key mechanisms implemented in AMPT, such as the parton cascade and hadronic rescattering, work on the elliptic anisotropy in small collision systems. In addition, various nonflow subtraction methods which exhibit different sensitivity to jet-like correlations are studied in this work.

II. MODEL AND METHODOLOGY

A multiphase transport model

The string melting version of AMPT model (v2.26t9b, available online)[32, 34] is employed in this study to calculate the v_2 of final-state particles in high-multiplicity p-Pb at 5.02 TeV. Four main processes are included in AMPT model: the initial conditions, the parton scatterings, hadronization and the hadronic interactions. The initial conditions are generated from the heavy ion jet interaction generator (HIJING) model[35, 36], where the minijet partons and soft excited string are produced, then they are converted to primordial hadrons based on the LUND fragmentation. Under the string melting mechanism, these primordial hadrons are melted into partons according to their flavor and spin structures. The elastic scatterings between the partons are simulated using the Zhang's parton cascade (ZPC) model[37], which includes two-body scatterings with the cross section described by the following simplified equation:

$$\sigma_{gg} \approx \frac{9\pi\alpha_s^2}{2\mu^2}. \quad (2)$$

In this paper, the strong coupling constant α_s is set to 0.33 and the Debye screening mass $\mu = 2.2814 \text{ fm}^{-1}$, then the total parton scattering cross section is $\sigma = 3 \text{ mb}$. In order to isolate the effect from partonic scattering, the σ is also set to be close to 0 by increasing μ in this work (see set "w/o parton scat." in Tab. I). After partons stop interacting with each other, the hadronization with a quark coalescence model is implemented to combine nearest two (or three) quarks into mesons (or baryons) [32]. The formed hadrons enter the subsequent hadronic rescattering process based on a relativistic transport (ART) model [38], where both elastic and inelastic scatterings are considered for baryon-baryon, baryon-meson, and meson-meson interactions. The hadronic interactions time is set to $t_{max} = 30 \text{ fm}/c$ by default. Alternatively, the t_{max} is set to 0.4 fm/c to effectively turns off the hadron scattering process but includes the resonance decay[39](see set "w/o hadron scat." in Tab. I). In addition, the random orientation of reaction plane is turn on and the shadowing effect is considered in this analysis.

Table I. Details of three configurations

Description	$\sigma(\text{mb})$	$t_{\text{max}}(\text{fm}/c)$
w/ all	3	30
w/o parton scat.	~ 0	30
w/o hadron scat.	3	0.4

Two-particle correlation and nonflow subtraction

The two-particle correlation method (2PC) is widely used to extract the flow(-like) signal in small collision system since it has great power to suppress the nonflow contribution from the long-range jet correlations. Similar to Eq. 1, the two particle azimuthal correlation of N^{pairs} emitted particle pairs (labeled as $C(\Delta\varphi)$) as a function of relative angle $\Delta\varphi = \varphi^a - \varphi^b$ between particle a and particle b can be expanded in a Fourier series as:

$$C(\Delta\varphi) = \frac{dN^{\text{pair}}}{d\Delta\varphi} \propto 1 + 2 \sum_{n=1}^{\infty} V_{n\Delta}(p_{\text{T}}^a, p_{\text{T}}^b) \cos[n(\Delta\varphi)], \quad (3)$$

where the $V_{n\Delta}$ is the two-particle n -th order harmonic. In a pure hydrodynamic picture, due to the particle emission is independent, the $V_{n\Delta}(p_{\text{T}}^a, p_{\text{T}}^b)$ can be factorized into product of single particle flow v_n^a and v_n^b :

$$V_{n\Delta}(p_{\text{T}}^a, p_{\text{T}}^b) = v_n(p_{\text{T}}^a) v_n(p_{\text{T}}^b). \quad (4)$$

Based on the factorization assumption, the v_n of single particle a can be obtained with so-called $3 \times 2\text{PC}$ method, which was recently proposed in PHENIX Collaboration[40]. It requires to form the two-particle correlations between three groups of particles (labeled as a , b and c) and extract the flow coefficients for three combinations:

$$v_n(p_{\text{T}}^a) = \sqrt{\frac{V_{n\Delta}(p_{\text{T}}^a, p_{\text{T}}^b) V_{n\Delta}(p_{\text{T}}^a, p_{\text{T}}^c)}{V_{n\Delta}(p_{\text{T}}^b, p_{\text{T}}^c)}}. \quad (5)$$

The main nonflow contribution to flow signal in small collision systems is from the jet correlations, which are classified into two parts: the near-side jet and away-side jet (dijet). The former is usually removed by applying large rapidity gap between trigger and associated particles when the correlations are constructed. The later one can be suppressed by introducing an estimation in low-multiplicity events with several methods. The traditional method is to subtract the correlation function distribution directly obtained in low-multiplicity events ("peripheral collisions") from that in high-multiplicity events ("central collisions"), assuming that both yield and shape of dijet are identical in central and peripheral collisions, as shown:

$$\begin{aligned} C^{\text{HM}}(\Delta\varphi) - C^{\text{LM}}(\Delta\varphi) &\propto 1 + 2 \sum_{n=1}^{\infty} V_{n\Delta} \cos[n(\Delta\varphi)] \\ &= a_0 + 2 \sum_{n=1}^{\infty} a_n \cos[n(\Delta\varphi)], \end{aligned} \quad (6)$$

where $C^{\text{HM}}(\Delta\varphi)$ and $C^{\text{LM}}(\Delta\varphi)$ represent the correlation function distribution obtained in low- and high-multiplicity events, respectively. This method relies on

the "zero yield at minimum" (ZYAM) hypothesis to subtract a flat combinatoric component from the correlation function in low-multiplicity events. So the fit parameter a_2 is the absolute modulation in the subtracted correlation function distribution and characterizes a modulation relative to a baseline assuming that such a modulation is not present in the low-multiplicity class below the baseline. In this case, the flow coefficient $V_{n\Delta}$ is calculated as:

$$V_{n\Delta} = a_n / (a_0 + b), \quad (7)$$

where b is the baseline estimated at the minimum of correlation function in low-multiplicity events. However the measurement of jet-like correlations in p-Pb collisions indicates that the dependence of dijet yield on particle multiplicity can not be ignored. In this case, a new template fit method is developed by the ATLAS collaboration, where the correlation function distribution obtained in high-multiplicity events, is assumed to result from a superposition of the distribution obtained in low-multiplicity events scaled up by a multiplicative factor F , and a constant modulated by $\cos(n\Delta\varphi)$ for $n > 1$, as shown in:

$$C(\Delta\varphi) = F C^{\text{LM}}(\Delta\varphi) + G \left(1 + 2 \sum_{n=1}^3 V_{n\Delta} \cos(n\Delta\varphi) \right), \quad (8)$$

where G is the normalization factor to keep the integral of $C(\Delta\varphi)$ is equal to $C^{\text{HM}}(\Delta\varphi)$. It is worth to noting that the ZYAM assumption is not considered in the default template fit method. In order to further characterize the influence of ZYAM assumption on the flow extraction, results obtained with an alternative version of the template fitting, so-called "template fit (ZYAM)", where a ZYAM procedure is performed by replacing $C^{\text{LM}}(\Delta\varphi)$ with $C^{\text{LM}}(\Delta\varphi) - C^{\text{LM}}(0)$ in Eq. 8, are also presented in this paper. Furthermore, an improved template fit method developed in recent years is also tested in this work. It applies a correction procedure on the default template fit method by considering the multiplicity dependence of remaining ridge in low-multiplicity events, as shown in:

$$V_{n\Delta} = V_{n\Delta}(\text{tmp}) - \frac{F G^{\text{LM}}}{G^{\text{HM}}} (V_{n\Delta}^2(\text{tmp}) - V_{n\Delta}^2(\text{LM})), \quad (9)$$

where the $V_{n\Delta}(\text{tmp})$ and $V_{n\Delta}^2(\text{LM})$ are obtained with default template method in high- and low-multiplicity events. All these nonflow subtraction methods are implemented in this work, and their different sensitivity on nonflow effect are also discussed in this paper.

III. ANALYSIS PROCEDURES

In order to compare the AMPT calculations with the results from ALICE directly, we focus on the particles are selected at pseudorapidity range $|\eta| < 0.8$ which is same as the TPC acceptance in ALICE. In 3×2 PC method, the long-range correlations are constructed between the charged particles at midrapidity, forward rapidity ($2.5 < \eta < 4$) and backward rapidity ($-4 < \eta < -2.5$), i.e. the central-forward correlation ($-4.8 < \Delta\eta < -1.7$), central-backward correlation ($1.7 < \Delta\eta < 4.8$) and backward-forward correlations ($-8 < \Delta\eta < -5$). In addition, the centrality classes are defined counting charged particles in the acceptance of the V0A detector, i.e. in $2.8 < \eta < 5.1$.

The correlation function distribution $C(\Delta\varphi)$ is obtained by correcting the number of particle-pairs in same events normalized to the number of trigger particles N_{trig} with event-mixing technique, as:

$$C(\Delta\varphi, \Delta\eta) = \frac{1}{N_{\text{trig}}} \frac{d^2 N_{\text{pairs}}}{d\Delta\eta d\Delta\varphi} = \frac{S(\Delta\varphi, \Delta\eta)}{B(\Delta\varphi, \Delta\eta)}, \quad (10)$$

where $S(\Delta\varphi, \Delta\eta) = \frac{1}{N_{\text{trig}}} \frac{d^2 N_{\text{same}}}{d\Delta\eta d\Delta\varphi}$ is the correlation function in same events and $B(\Delta\varphi, \Delta\eta) = \alpha \frac{d^2 N_{\text{mixed}}}{d\Delta\eta d\Delta\varphi}$ is the associated yield as a function of $\Delta\varphi$ and $\Delta\eta$ in mixed events. The factor α is used to normalize the $B(\Delta\varphi, \Delta\eta)$ to unity in the $\Delta\eta$ region of maximal pair acceptance. The obtained 2-D correlation function $C(\Delta\varphi, \Delta\eta)$ is projected into $\Delta\varphi$ axis, then we follow the nonflow subtraction procedures and factorization as discussed in Eq. 5–Eq. 9, the v_2 of charged particles at $|\eta| < 0.8$ can be calculated.

IV. RESULTS AND DISCUSSIONS

We investigate the effects from partonic and hadronic cascade on the p_T spectrum of identified particles before performing the flow analysis. Figure 1 shows the p_T distribution of proton, pion and kaon in 0–20% high-multiplicity p–Pb collisions at $\sqrt{s_{\text{NN}}} = 5.02$ TeV, obtained from AMPT using three set of configurations listed in Tab. I, and the experimental data from ALICE. The AMPT results with and without considering hadronic rescatterings are consistent with each other. This behavior is different from the previous findings in heavy-ion collisions where the hadronic interaction reduce the particle yield significantly [41]. In contrast, the spectrum obtained in AMPT without considering the parton cascade process is enhanced compared to that with partonic scattering, and such enhancement is more significant at high p_T . This outcome is expected, as partons experience energy loss during the

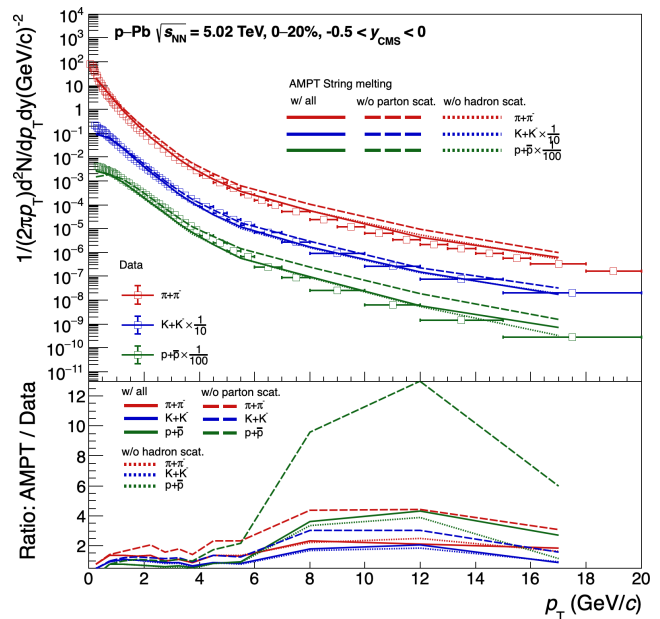


Figure 1. The p_T distribution of pions, kaons and protons in 0–20% high-multiplicity p–Pb collisions at $\sqrt{s_{\text{NN}}} = 5.02$ TeV, obtained from AMPT model calculations, is compared to ALICE measurement. The results in AMPT without hadronic scattering and partonic scattering are also presented.

parton cascade, which reduces the production of final-state particles. In addition, the ratios of the p_T spectra obtained from AMPT calculations and data are also shown. The AMPT model calculation with both partonic and hadronic scattering can well reproduce the data at intermediate and low p_T , but slightly overestimate the data at high p_T , due to the absence of inelastic parton collisions and subsequently fragmentation for hard partons [34].

Figure 2 (left) shows the v_2 of pions, kaons, protons and Λ as a function of p_T in 0–20% high-multiplicity p–Pb collisions at $\sqrt{s_{\text{NN}}} = 5.02$ TeV, obtained in AMPT calculations with 3×2 PC method. The comparison with the ALICE measurement for the v_2 of charged hadrons, pions, kaons and protons, and the CMS measurement for the v_2 of K_s^0 and Λ , is also presented. In AMPT calculations, the away-side jet contribution is suppressed by applying the template fit method and the ZYAM assumption is considered in order to compare with data directly. A positive v_2 of charged hadrons, pions, kaons, protons and Λ is observed in AMPT calculations, and the mass ordering effect (i.e. the v_2 of baryons is lower than that of mesons) is also reproduced for $p_T < 2$ GeV/c. These features indicate that the particle production from a collective expanding source observed in data is generated also in AMPT model. Thanks to

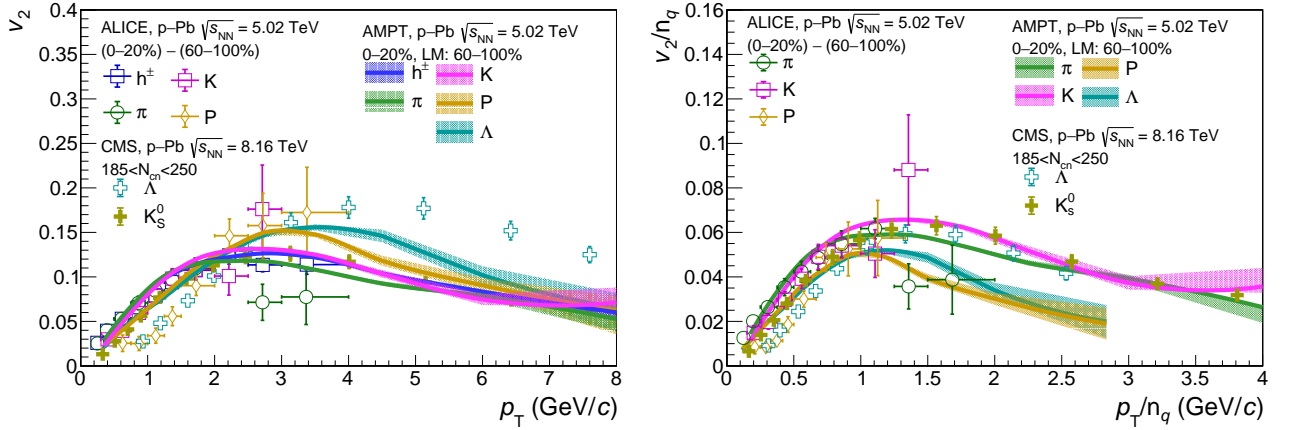


Figure 2. Left: the v_2 as a function of p_T in 0–20% high-multiplicity p–Pb collisions at $\sqrt{s_{NN}} = 5.02$ TeV, obtained from default AMPT model calculations with $3\times 2PC$ method, is compared to ALICE and CMS measurement. Right: the p_T -differential v_2 scaled by the number of constituent quark (n_q).

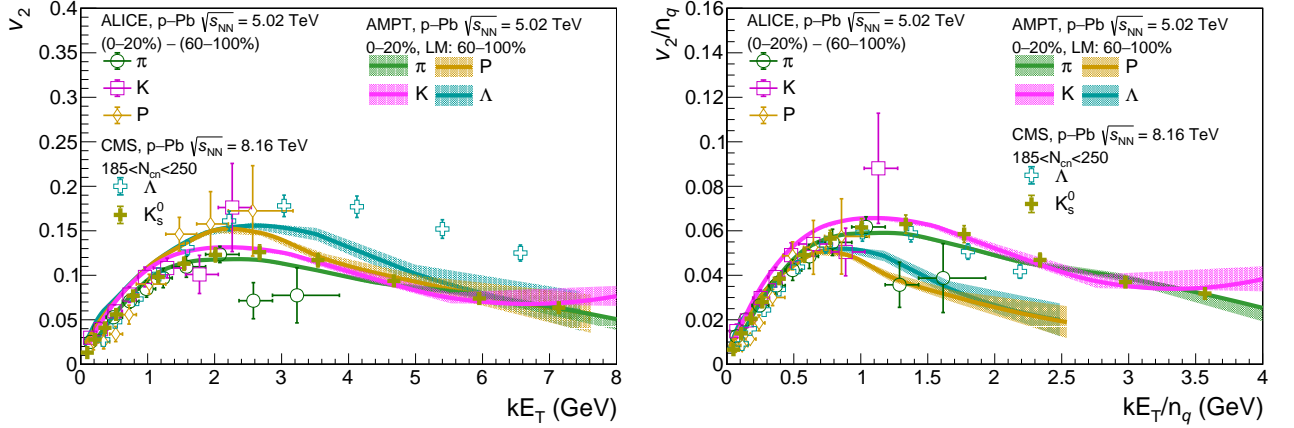


Figure 3. Left: the v_2 as a function of transverse kinetic energy (kE_T) in 0–20% high-multiplicity p–Pb collisions at $\sqrt{s_{NN}} = 5.02$ TeV, obtained from default AMPT model calculations with $3\times 2PC$ method, is compared to ALICE and CMS measurement. Right: the kE_T -differential v_2 scaled by the number of constituent quark (n_q).

the advanced flow extraction method, the calculations of v_2 in AMPT is firstly extended to high p_T region, up to 8 GeV/c. The v_2 of protons and Λ are consistent, and both of them are higher than v_2 of mesons for $2 < p_T < 7$ GeV/c. Such so-called meson-baryon particle type grouping, which was widely observed in flow measurement in heavy-ion collisions, hints the collective behavior at the partonic level followed by quark coalescence into hadrons. This grouping can be further studied by using the number of constituent quarks (NCQ) scaling technique, as described in [21]. The v_2 and p_T in Fig. 2 (left) are replaced by v_2/n_q and p_T/n_q , where the n_q is the number of constituent quark in mesons ($n_q = 2$) and baryons ($n_q = 3$), as shown in Fig. 2 (right). The v_2/n_q obtained from data shows

an approximative NCQ scaling of v_2 at intermediate p_T , but the results calculated in AMPT can not reproduce the scaling in $1 < p_T/n_q < 2$ GeV/c. It may be attributed to the hadronization mechanism implemented in current AMPT version, where the baryons are produced only after the formation of meson according simply combining three nearest partons regardless of the relative momentum among the coalescing partons [42]. Furthermore, we also plot the v_2 of identified particle as a function of the transverse kinetic energy kE_T ($kE_T = m_T - m_0 = \sqrt{p_T^2 + m_0^2} - m_0$), as shown in Fig. 3 (left). Different from the mass ordering effect observed in Fig. 2 (left), all particle species scale to a common set of v_2 values for $kE_T \lesssim 1$ GeV, confirming the similar influence of a collective expanding source in

both data and AMPT. Figure 2 (right) shows the results obtained after NCQ scaling of the v_2 values shown in Fig. 2 (left), where v_2 and kE_T are divided by the number of constituent quark n_q . Similarly, the data shows a good scaling over the full range of kE_T values, indicating the quark degree of freedom in the flowing matter, while the AMPT results underestimate the baryon v_2 for $p_T > 2\text{GeV}/c$. More studies on v_2 calculations in small collision systems with improved quark coalescence model in AMPT need to be performed in the future.

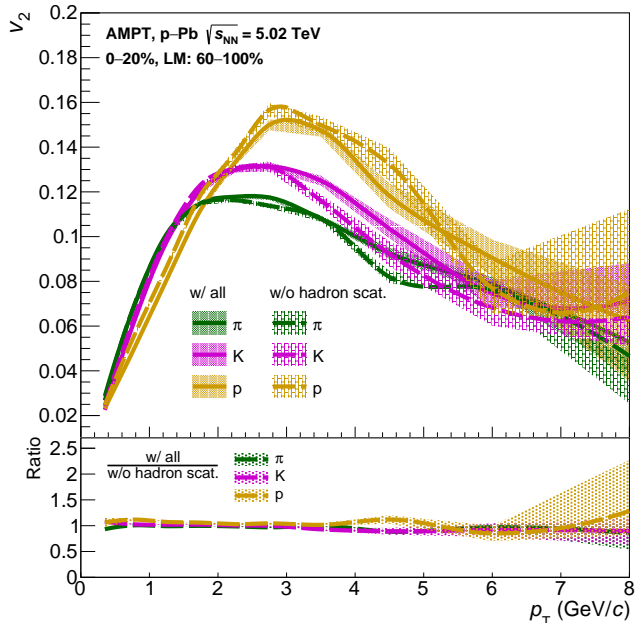


Figure 4. The p_T -differential v_2 of pions, kaons and protons calculated in AMPT model with and without considering hadronic scattering. The ratio of two sets are also presented.

The effects of partonic and hadronic scatterings on elliptic anisotropy of final-state particles are also examined in this work. Figure 4 displays the calculated v_2 of pions, kaons and protons in AMPT with and without considering hadronic rescattering process. The results show that the ratio between the v_2 values with and without hadron rescattering is consistent with unity for all particle species, indicating that the hadronic rescattering mechanism has almost no effect on v_2 . When we turn off the parton scattering in AMPT, i.e. the parton scattering cross section $\sigma = 0$, the $V_{2\Delta}$ of charged particles for central-forward (CF) and central-backward (CB) correlations is almost zero, as shown in Fig. 5. It proves that the elliptic anisotropy in high-multiplicity small collision systems is mostly generated by parton scatterings. This conclusion is consistent with previous studies in AMPT [33], which suggests that few parton scatterings in small collision systems are sufficient to generate significant elliptic anisotropies through the

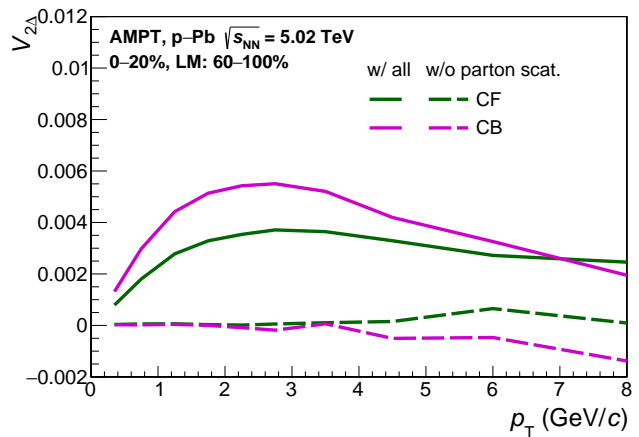


Figure 5. The p_T -differential $V_{2\Delta}$ for central-forward (CF) and central-backward (CB) correlations calculated in AMPT model with and without considering partonic scattering.

parton escape mechanism.

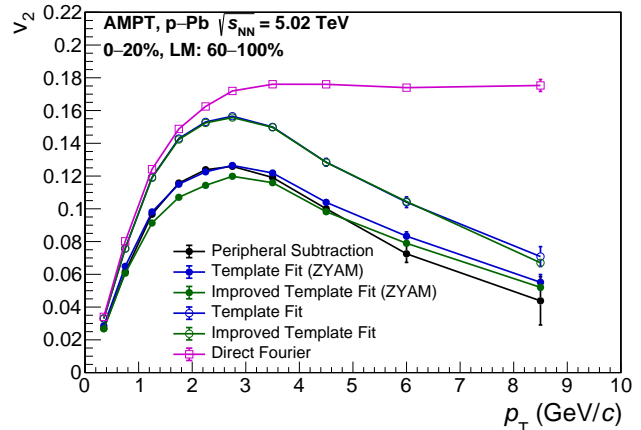


Figure 6. The p_T -differential v_2 of charged particles calculated in AMPT with different nonflow subtraction methods.

Different nonflow subtraction methods are also investigated in this paper. Figure 6 (left) shows the p_T -differential v_2 of charged particles calculated with 3 \times 2PC method in 0–20% high-multiplicity p–Pb collisions, and several nonflow subtraction methods are implemented. In order to demonstrate how the nonflow contribution is removed, the v_2 obtained with a direct Fourier transform of the $C(\Delta\varphi)$ correlation (as shown in Eq. 3) is also presented. The results with all subtraction methods are suppressed significantly, especially at high- p_T where the jet correlations dominate. The results obtained with peripheral subtraction and template fit are consistent under the ZYAM hypothesis, indicat-

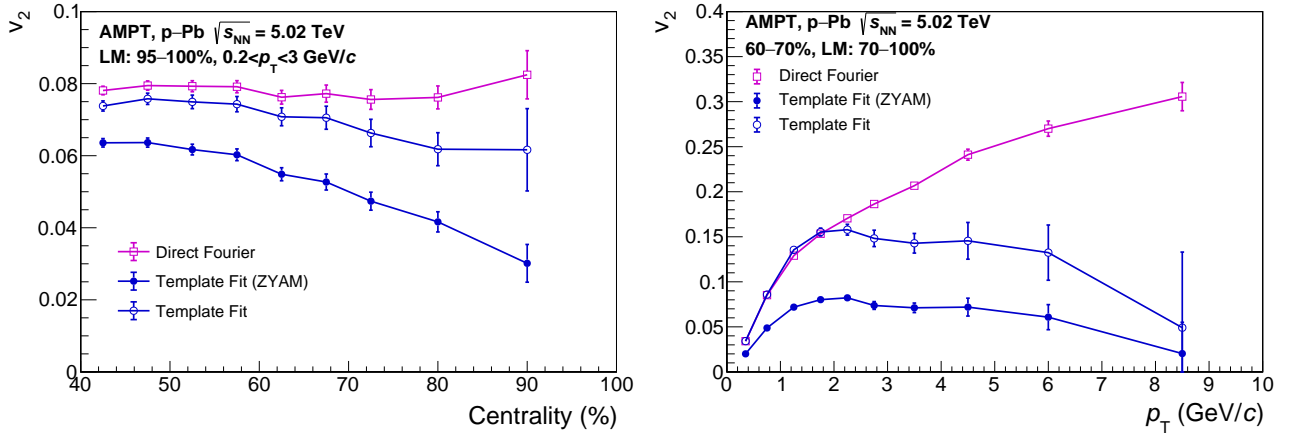


Figure 7. Left: the v_2 of charged particles in $0.2 < p_T < 3$ GeV/c as a function of centrality in p–Pb collisions at 5.02 TeV from AMPT calculations. Right: the p_T -differential v_2 of charged particles in 60–70% p–Pb collisions at 5.02 TeV from AMPT calculations. The template fit with and without ZYAM assumption, and the direct Fourier transform are all performed.

ing that the away-side jet contribution is automatically removed with the 3×2 PC method even the dependence of jet correlation on multiplicity is not considered in peripheral subtraction method. The v_2 calculated with improved template fit method is slightly lower than that from template fit, and it is similar to the features observed in ATLAS measurement [43]. On the other hand, all results without considering ZYAM assumption (i.e. the default template fit and improved template fit method) are systematically higher than that with ZYAM assumption. It is expected since the baseline is not introduced when the v_2 is extracted from $V_{2\Delta}$, as described in Eq. 7.

We further investigate the applicability of ZYAM assumption in nonflow subtraction in small collision systems. Figure 7(left) shows the v_2 of charged particles as a function of centrality, with the p_T selection $0.2 < p_T < 3$ GeV/c. The template fit, ZYAM-based fit and the direct Fourier transform are performed to extract the v_2 signal. The v_2 obtained with template fit is nearly independent of centrality, implying that the long-range correlation is also present at very low multiplicity, as concluded in Ref [44]. The comparison with the v_2 obtained with ZYAM-based fitting, which decrease with increasing centrality, illustrates the improvement brought about in the template fitting procedure. The v_2 obtained with both template fit and ZYAM-based fit methods are lower than that from direct Fourier transform. However, the default template fit method also has the limitation to estimate the magnitude of v_2 . Figure 7 (right) shows the p_T -differential v_2 of charged particles in 60–70% p–Pb collisions at 5.02 TeV from AMPT calculations. Compared to the results calculated without nonflow subtraction (i.e. the direct

Fourier transform), the v_2 obtained with default template fit method is even higher below $p_T < 2.5$ GeV/c. These results indicate that default template fit method and ZYAM-based methods may correspond to the upper and lower limit of the nonflow subtraction in small collision systems and both of them should be carefully considered in the future measurements.

V. SUMMARY

We studied the elliptic anisotropy of identified particles (pions, kaons, protons and Λ) in high-multiplicity p–Pb collisions at 5.02 TeV with the AMPT model. The p_T -differential v_2 of mesons can be reasonably described, while the baryon v_2 is slightly overestimated. A clear mass ordering effect is found below the p_T of 2 GeV/c, which indicates that the hydro-like behavior can be well reproduced by via parton escaping. We also extend the calculation of v_2 to higher p_T region up to 8 GeV/c in AMPT for the first time, and examine the baryon-meson grouping driven by the quark coalescence as well as their approximate NCQ scaling. In particular, we demonstrate that the parton interactions can simultaneously reduce the production of light hadrons and fully contribute their v_2 , while the hadronic rescatterings has almost no influence on the elliptic anisotropy of final-state particles. In addition, a detailed investigation about the flow extraction methods and several nonflow subtraction techniques with AMPT, is also performed in this work. We argue that the 3×2 PC method has the better capability for suppressing the near-side jet contribution and refraining from the break of factorization. The different sensitivity exhibited by vari-

ous subtraction methods to nonflow effects are also discussed. We found that default template fit and ZYAM-based method both have shortcoming for subtracting the away-side jet correlations, which need to be carefully considered in future measurements in small collision systems.

VI. ACKNOWLEDGEMENT

This work was supported by Natural Science Foundation of Hubei Provincial Education Department under Grant (Q20131603) and Key Laboratory of Quark and Lepton Physics (MOE) in Central China Normal University under Grant (QLPL2022P01, QLPL202106).

-
- [1] E. V. Shuryak, Phys. Lett. B **78**, 150 (1978).
 - [2] E. V. Shuryak, Phys. Rept. **61**, 71 (1980).
 - [3] J.-Y. Ollitrault, Phys. Rev. D **46**, 229 (1992).
 - [4] S. A. Voloshin, Nucl. Phys. A **827**, 377C (2009).
 - [5] S. Voloshin and Y. Zhang, Z. Phys. C **70**, 665 (1996).
 - [6] A. M. Poskanzer and S. A. Voloshin, Phys. Rev. C **58**, 1671 (1998).
 - [7] B. Alver and G. Roland, Phys. Rev. C **81**, 054905 (2010), [Erratum: Phys.Rev.C 82, 039903 (2010)].
 - [8] B. H. Alver, C. Gombeaud, M. Luzum, and J.-Y. Ollitrault, Phys. Rev. C **82**, 034913 (2010).
 - [9] G.-Y. Qin, H. Petersen, S. A. Bass, and B. Muller, Phys. Rev. C **82**, 064903 (2010).
 - [10] D. Teaney and L. Yan, Phys. Rev. C **83**, 064904 (2011).
 - [11] I. Arsene *et al.* (BRAHMS), Nucl. Phys. A **757**, 1 (2005).
 - [12] K. Adcox *et al.* (PHENIX), Nucl. Phys. A **757**, 184 (2005).
 - [13] B. B. Back *et al.* (PHOBOS), Nucl. Phys. A **757**, 28 (2005).
 - [14] J. Adams *et al.* (STAR), Nucl. Phys. A **757**, 102 (2005).
 - [15] K. Aamodt *et al.* (ALICE), Phys. Rev. Lett. **107**, 032301 (2011).
 - [16] S. Acharya *et al.* (ALICE), JHEP **07**, 103 (2018).
 - [17] G. Aad *et al.* (ATLAS), Phys. Rev. C **86**, 014907 (2012).
 - [18] S. Chatrchyan *et al.* (CMS), Phys. Rev. C **89**, 044906 (2014).
 - [19] arXiv e-prints (2022), 10.48550/arXiv.2206.04587.
 - [20] S. Acharya *et al.* (ALICE), JHEP **10**, 152 (2021).
 - [21] D. Molnar and S. A. Voloshin, Phys. Rev. Lett. **91**, 092301 (2003).
 - [22] Z.-w. Lin and D. Molnar, Phys. Rev. C **68**, 044901 (2003).
 - [23] S. Chatrchyan *et al.* (CMS), Phys. Lett. B **718**, 795 (2013).
 - [24] B. Abelev *et al.* (ALICE), Phys. Lett. B **719**, 29 (2013).
 - [25] G. Aad *et al.* (ATLAS), Phys. Rev. Lett. **110**, 182302 (2013).
 - [26] B. B. Abelev *et al.* (ALICE), Phys. Lett. B **726**, 164 (2013).
 - [27] P. Bozek, Phys. Rev. C **85**, 014911 (2012).
 - [28] P. Bozek and W. Broniowski, Phys. Lett. B **718**, 1557 (2013).
 - [29] J. L. Nagle and W. A. Zajc, Ann. Rev. Nucl. Part. Sci. **68**, 211 (2018).
 - [30] K. Dusling and R. Venugopalan, Phys. Rev. D **87**, 094034 (2013).
 - [31] K. Dusling and R. Venugopalan, Phys. Rev. D **87**, 051502 (2013).
 - [32] Z.-W. Lin, C. M. Ko, B.-A. Li, B. Zhang, and S. Pal, Phys. Rev. C **72**, 064901 (2005).
 - [33] L. He, T. Edmonds, Z.-W. Lin, F. Liu, D. Molnar, and F. Wang, Phys. Lett. B **753**, 506 (2016).
 - [34] Z.-W. Lin and L. Zheng, Nucl. Sci. Tech. **32**, 113 (2021).
 - [35] X.-N. Wang and M. Gyulassy, Phys. Rev. D **44**, 3501 (1991).
 - [36] M. Gyulassy and X.-N. Wang, Comput. Phys. Commun. **83**, 307 (1994).
 - [37] B. Zhang, Comput. Phys. Commun. **109**, 193 (1998).
 - [38] B.-A. Li and C. M. Ko, Phys. Rev. C **52**, 2037 (1995).
 - [39] L. Zheng, H. Li, H. Qin, Q.-Y. Shou, and Z.-B. Yin, Eur. Phys. J. A **53**, 124 (2017).
 - [40] N. J. Abdulameer *et al.* (PHENIX), Phys. Rev. C **107**, 024907 (2023).
 - [41] Z.-w. Lin, S. Pal, C. M. Ko, B.-A. Li, and B. Zhang, Phys. Rev. C **64**, 011902 (2001).
 - [42] Y. He and Z.-W. Lin, Phys. Rev. C **96**, 014910 (2017).
 - [43] M. Aaboud *et al.* (ATLAS), Phys. Lett. B **789**, 444 (2019).
 - [44] G. Aad *et al.* (ATLAS Collaboration), Phys. Rev. Lett. **116**, 172301 (2016).